

1 **Association of Human Mobility and Weather Conditions with Dengue Mosquito**
2 **Abundance during the COVID-19 Pandemic in Hong Kong**

3

4

Yufan Zheng^{a,b}, Keqi Yue^{a,c}, Eric W. M. Wong^b, Hsiang-Yu Yuan^{a,d,*}

5

6 ^aDepartment of Biomedical Sciences, Jockey Club College of Veterinary Medicine and Life
7 Sciences, City University of Hong Kong, Hong Kong SAR, China

8 ^bDepartment of Electrical Engineering, College of Engineering, City University of Hong
9 Kong, Hong Kong SAR, China

10 ^cDepartment of Chronic Disease Epidemiology, Yale School of Public Health, New Haven,
11 CT, United States

12 ^dCentre for Applied One Health Research and Policy Advice, Jockey Club College of
13 Veterinary Medicine and Life Sciences, City University of Hong Kong, Hong Kong SAR,
14 China

15 *Correspondence: sean.yuan@cityu.edu.hk

16

17 **ABSTRACT**

18 **Background**

19 While *Aedes* mosquitoes, the Dengue vectors, were expected to expand their spread due to
20 international travel and climate change, the effects of human mobility and low rainfall
21 conditions on them are largely unknown. We aimed to assess these influences during the
22 COVID-19 pandemic in Hong Kong, characterized by varying levels of human mobility.

23
24 **Methods**

25 Google's human mobility indices (including residential, parks and workplaces) and weather
26 conditions (total rainfall and mean temperature) together with *Aedes albopictus* abundance
27 and extensiveness monitored using Gravidtrap were obtained between April 2020 and August
28 2022. Distributed lag non-linear models with mixed-effects models were used to explore their
29 influence in three areas in Hong Kong.

30
31 **Findings**

32 The relative risk (RR) of mosquito abundance was associated with low rainfall (<50 mm)
33 after 4.5 months, with a maximum of 1.73, compared with 300 mm. Heavy rainfall (>500
34 mm) within 3 months was also associated with a peak of RR at 1.41. Warm conditions (21-
35 30°C; compared with 20°C) were associated with a higher RR of 1.47 after half a month.
36 Residential mobility was negatively associated with mosquito abundance. The model
37 projected that if residential mobility in the year 2022 was reduced to the level before the
38 COVID-19 pandemic, the mosquito abundance would increase by an average of 80.49%
39 compared to the actual observation.

40
41 **Significance**

42 Both the human mobility and the lag effect of meteorological factors can be critical for the
43 prediction of vector dynamics, and stay-at-home policy may be useful for its control in
44 certain regions.

45

46 **AUTHOR SUMMARY**

47 Previous studies have demonstrated that both meteorological factors and human mobility
48 were linked to the risk of Dengue transmission, with rainfall potentially exerting delayed
49 effects. Moreover, dry conditions have been found to increase Dengue risk in recent years.
50 However, the impact of these factors on vector (mosquito) activity remains unclear. This
51 study assessed the effect of human mobility and rainfall on the Dengue mosquito. The
52 Gravitrap indices were used to characterize local mosquito (*Aedes Albopictus*) abundance and
53 extensiveness conditions. We used established Gravitrap indices to characterize mosquito
54 abundance and extensiveness in Hong Kong. We found that i) the decrease in residential
55 mobility might increase mosquito abundance and extensiveness; and ii) low rainfall (<50 mm)
56 was associated with a higher risk of mosquito abundance after 4.5 months. Additionally,
57 heavy rainfall was associated with increased mosquito activity risk. The future mosquito
58 activity risk is expected to increase because of the relaxation of social distancing measures
59 after the COVID-19 pandemic along with climate change. The results suggest that non-linear
60 delayed effects of meteorological factors together with human mobility change can be used
61 for the Dengue mosquito forecast. Social distancing may be a way to reduce the risk of *Aedes*
62 *albopictus*.

63 **INTRODUCTION**

64 Dengue fever (DF) is one of the most widespread mosquito-borne diseases, with an estimated
65 390 million infections each year (1). *Aedes aegypti* and *Aedes albopictus* are two Dengue
66 vectors. Global warming can facilitate their spread, leading to increasing risk in certain
67 previously non-endemic subtropics, including southern China (2). In addition, according to a
68 recent study, the risk of DF incidence can also be largely influenced by social distancing
69 measures and human movement behaviours (3). Hong Kong, a metropolitan in southern
70 China, faces an increased risk of Dengue outbreaks (4). Understanding how human mobility
71 together with weather conditions affects *Aedes* mosquito abundance in Hong Kong helps
72 make an early assessment of Dengue risk and decision-making in vector control.

73

74 In response to the increasing risk of DF (4), Hong Kong has established a Gravidtrap system
75 for vector surveillance since 2020 to replace the Ovitrap. The Gravidtrap was developed to
76 capture female *Aedes Albopictus* (5). In addition to the extensiveness (i.e. the distribution) of
77 *Aedes Albopictus*, which could be measured by both traps, the new trap also monitored the
78 abundance (i.e. the number) of mosquitoes.

79

80 During 2020 and 2022, social distancing was regularly introduced to reduce the spread of
81 COVID-19. In 2022, strict social distancing was introduced during the COVID-19 Omicron
82 wave. The strict social distancing might affect the likelihood of mosquitoes biting humans,
83 especially *Aedes albopictus*, which tends to stay outside (6). Therefore, incorporating human
84 mobility into mosquito prediction modelling is essential, especially when social distancing is
85 implemented.

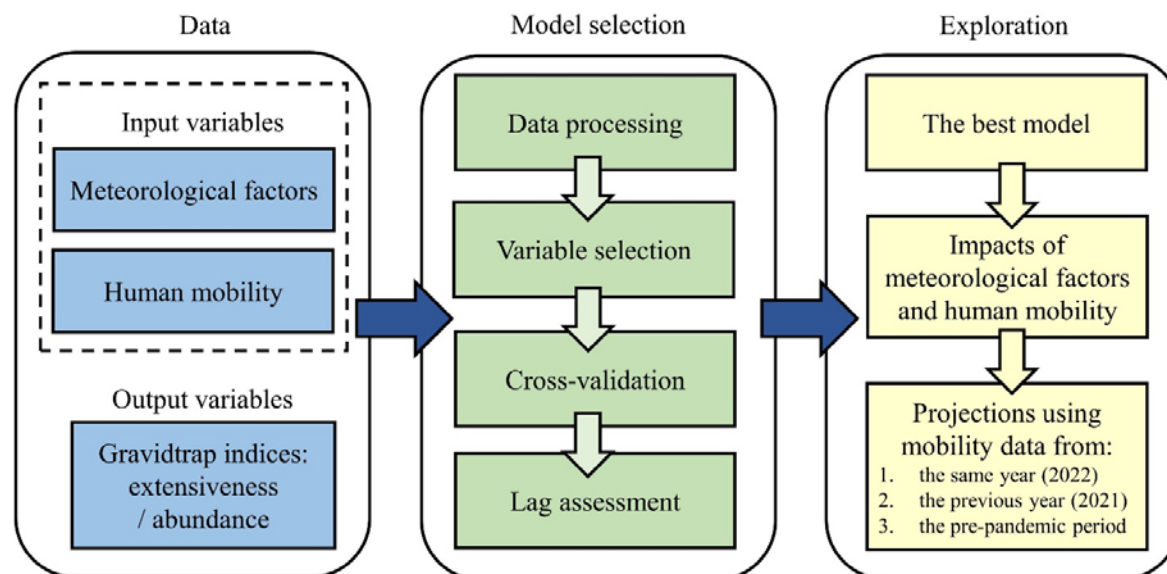
86

87 While a warm condition has a known impact on mosquito development, breeding, survival,
88 etc., (7) the effects of rainfall are diverse, with both heavier and lower rainfall being
89 associated with increased Dengue risk. Rainfall was an important Dengue risk factor (1,8),
90 but recent studies found that drought conditions were also associated with a higher risk of
91 Dengue incidence at long lead times of up to 5 months (9,10). Similarly, springtime rainfall, a
92 few months before seasonal Dengue outbreaks, appeared to be negatively associated with
93 annual Dengue incidence in Taiwan and Hong Kong (4,11). These previous studies suggested
94 a varied relationship between hydroclimatic factors and Dengue incidence with delay effects
95 (4,9–11). However, whether these delay effects occurred through influencing mosquito
96 population dynamics remains largely unknown.

97

98 Our study aimed to assess the influence of human mobility on the abundance and
99 extensiveness of *Aedes albopictus*, taking account of the nonlinear lagged effects of total
100 rainfall and mean temperature (Figure 1). The results provided important insights for Dengue
101 risk prediction and control.

102



103

104

105 **Figure 1 Schematic flow for exploration of different factors in the mosquito**
106 **extensiveness and abundance predictions.** WAIC was used for variable selection. The best
107 model was determined after the results were cross-validated and compared with different
108 lagged periods.

109

110 METHODS

111 Meteorological data

112 Meteorological data in Hong Kong were collected based on the weather stations in three
113 regions from the Hong Kong Observatory (12), including daily total rainfall and daily mean
114 temperature. We collected the data from April 2020 to August 2022 and divided it into three
115 areas (13): Hong Kong Island and Kowloon (HKK), New Territories East (NTE), and New
116 Territories West (NTW) (Table S1). Monthly total rainfall and monthly mean temperature (i.e.
117 obtained by averaging the daily mean temperatures) were calculated from these daily
118 measurements (Table S2). The meteorological factors for each area are the average value of
119 selected weather stations within that area (Supplementary Methods).

120

121 Human mobility data

122 Human mobility data for Hong Kong were collected from Google to represent the human
123 behavioural changes in response to the COVID-19 pandemic and social distance measures
124 during the study period (14). We used three categories of places in human mobility data,
125 including residential, parks and workplaces. All indices were computed relative to a baseline
126 day. The baseline day is the median value from the 5 weeks Jan 3–Feb 6, 2020. The monthly
127 human mobility index was calculated for model prediction (see Supplementary Methods).

128

129 Mosquito activity data

130 Mosquito activity data were provided by the Food and Environmental Hygiene Department
131 (15). Two indices were measured by the mosquito Gravidtrap surveillance: The Area Density
132 Index (ADI) defined as the number of mosquitoes captured in the traps (used to represent the
133 abundance of *Aedes albopictus*); and the Area Gravidtrap Index (AGI), defined as the
134 proportion of Gravidtraps that are found to have positive results in a specific area (used to
135 represent the extensiveness of *Aedes albopictus*).

136

137 We calculated the abundance and extensiveness for each area during each month t . First, the
138 index for each area (i.e. HKK, NTE, and NTW) was calculated as the average index for all
139 Gravidtrap sites in the region.

140

141 The average monthly mosquito extensiveness in area A is defined as:

142

$$143 \quad \overline{AGI}^A(t) = \sum_{m_i \in M^A(t)} (AGI^{m_i}(t)) / n_m^A(t) \quad (\text{eq. 1})$$

144

145 where n_m^A represents the total number of mosquito monitoring sites in area A . AGI^{m_i}
146 represents the AGI in the surveyed area m_i . $M^A = \{m_1, m_2, \dots, m_i\}$ is a collection of sites
147 (surveyed areas), in which m_i represents each site in the area.

148

149 The monthly abundance $N^A(t)$ (per 1,000 traps) in area A is defined as:

150

$$151 \quad N^A(t) = \sum_{m_i \in M^A(t)} (AGI^{m_i}(t) \cdot ADI^{m_i}(t) \cdot 1000) / n_m^A(t) \quad (\text{eq. 2})$$

152

153 where $ADI^{m_i}(t)$ represents the mean ADI at the site m_i in month t .

154

155 **Model development**

156 We developed prediction models for mosquito abundance and extensiveness based on
157 distributed-lagged non-linear models (DLNM) (16). For mosquito abundance prediction, we
158 assumed the mosquito number per 1000 traps follows the negative binomial distribution and
159 selected the log function as the link function. Let λ_t be the mosquito number per 1000 traps in
160 the month t , such as:

161

$$\lambda_t \sim NB(u_t, \kappa)$$

162

163 where u_t is distribution mean of λ_t at month t and κ is the overdispersion parameter in the
164 negative binomial distribution. λ_t in area, A can be measured by monthly mosquito
165 abundance $N^A(t)$ (see eq. 2). Then, the regression model to predict mosquito abundance was:

166

$$167 \quad \log(\lambda_t) = \beta + \gamma + S + f.w(R_t, l_1) + f.w(T_t, l_2) + m_t + \alpha \quad (\text{eq. 3})$$

168

169 where $f.w(R_t, l_1)$ and $f.w(T_t, l_2)$ represent the nonlinear exposure-lag functions of total
170 rainfall R_t from 0 to l_1 months and mean temperature T_t from 0 to l_2 months in t^{th} month,
171 respectively; S is the area random effect; γ is the monthly random effect; β is the yearly
172 random effect; α is the intercept; and m_t is the human mobility index in one category (e.g.
173 residential areas, workplaces, or parks) at t^{th} month.

174

175 In the mosquito extensiveness prediction, we assumed the number of positive traps follows
176 the binomial distribution and selected the logit function as the link function. Let Y_t be the
177 number of positive traps in the t^{th} month, following the binomial distribution with the total
178 number of the traps (n_t), and the probability of a positive trap (p_t) in the t^{th} month, such as:

179

$$Y_t \sim B(n_t, p_t)$$

180

181 where p_t at each surveyed area A can be measured by \overline{AGI}^A (see eq. 1). n_t can be calculated
182 as the product of the number of surveyed sites and the average number of traps per site. In
183 Hong Kong, an average of 55 Gravidtrap were placed in each selected site. Similarly, the
184 regression model to predict mosquito extensiveness was:

185

186

$$\text{logit}(p_t) = \beta + \gamma + S + f.w(R_t, l_1) + f.w(T_t, l_2) + m_t + \alpha \quad (\text{eq. 4})$$

187

188 **Model selection criteria**

189 To determine the best model (best-prediction model) among different combinations of
190 predictors, in a two-stage selection approach, the Watanabe-Akaike information criterion
191 (WAIC) was used in the first stage to select different sets of variables (candidate models)
192 (17). Besides the yearly, monthly, and area-specific random effects, variables include the lag
193 effects of total rainfall and mean temperature and three human mobility indices (see Table
194 S3) In the second stage, leave-one-out cross-validation (LOOCV) based on mean square
195 error (MSE) was performed for the candidate models to compare the model's predictions to
196 the observed data.. In LOOCV, the data set is divided into k parts (i.e. the total number of
197 months), where k-1 parts are used as the training set and the remaining parts are used as the
198 validation set. The procedure was repeated until every part (i.e. month) had been used for
199 validation.

200

201 **Comparison between mosquito abundance and extensiveness**

202 For comparing the predictive performance among mosquito abundance and extensiveness, we
203 used two standardized mosquito indices to unify the scales of different indices: the
204 standardized abundance index (SAI) and the standardized extensiveness index (SEI). The SAI
205 was:

206

$$SAI = \lambda / \sigma_\lambda$$

207

208 where λ and σ_λ represent mosquito abundance and standard deviation of mosquito abundance,
209 respectively. Similarly, the SEI was:

210

$$SEI = p / \sigma_p$$

211

212 where p and σ_p represent mosquito extensiveness and standard deviation of mosquito
213 extensiveness, respectively.

214 **RESULTS**

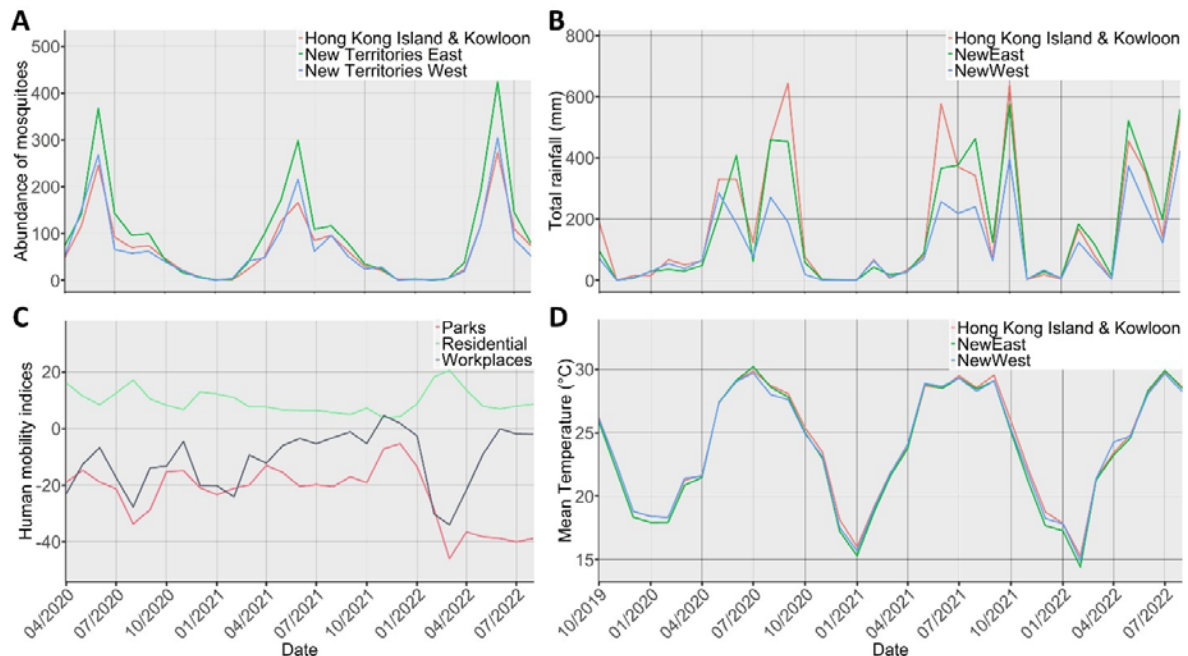
215 **Data analysis**

216 In Hong Kong, mosquito abundance exhibited strong seasonal patterns, growing in the spring
217 (March-May), peaking in the early summer (June or July), and remaining nearly at 0 in the
218 winter (December-February) (Figure 2A). Among three predefined regions, NTE (a
219 northeastern region) recorded higher mosquito abundance (i.e. the number of *Aedes*
220 *albopictus*) than others. Mosquito extensiveness (i.e. the distribution of *Aedes albopictus*) had
221 a similar pattern of variation to abundance (Figure S1 and Figure S2). Two mosquito
222 standardized indices were proposed for mosquito abundance and extensiveness prediction
223 (Figure S3). in Hong Kong from April 2020 to August 2022. During the study period, human
224 mobility generally fluctuated at the beginning but showed rapid declines in parks and
225 workplaces and a sharp increase in residential since January 2022. This rapid change
226 reflected the behavioural changes and social distancing measures introduced during the
227 COVID-19 Omicron wave (Figure 2B).

228

229 The monthly total rainfall typically exceeded 300mm during summer and early autumn (June-
230 October) and was mostly less than that during winter and early spring (November-April) but
231 varied substantially between different regions and years. For example, in 2020–2021, HKK (a
232 southern region) had the most total rainfall, while NTW (a northwestern region) had the least
233 (Figure 2C). In 2022, all the regions experienced higher levels of total rainfall in February
234 than the previous year. The monthly mean temperature among these three regions was similar,
235 with the highest at about 30°C around July and the lowest at about 15°C in January or
236 February (Figure 2D).

237



238

239

240 **Figure 2 The monthly change in mosquito abundance and its predictors in Hong Kong.**

241 (A) Mosquito abundance; (B) Total rainfall; (C) Human mobility; (D) Mean temperature. In

242 A, B, and D, red refers to Hong Kong Island and Kowloon (HKK); blue refers to New

243 Territories East (NTE); and green refers to New Territories West (NTW).

244

245

246

247 **Model selection of mosquito abundance and extensiveness**

248 After initial variable selection, a baseline model for mosquito abundance prediction (Model A;
 249 see Table 1) was obtained. The candidate models in mosquito abundance prediction (see eq. 3)
 250 include Model A, Model A-M_p, Model A-M_w, and Model A-M_r. After incorporating human
 251 human mobility in residential, the best model for abundance (Model A-M_r) was obtained using
 252 LOOCV. The best model for extensiveness (Model E-M_r) also contained the same set of
 253 variables.

254

255 **Table 1 Comparison of candidate models for mosquito abundance.**

256 The top six rows represent the results of variable selection to obtain the best model. The
 257 bottom six rows represent the results of sensitivity analysis to ensure the best time lag of
 258 total rainfall and mean temperature. Model A comprised the total rainfall with lags from 0 to
 259 6 months, mean temperature with lags from 0 to 2 months, and random effects for years,
 260 months, and regions were used as a baseline model. Model A-M_p, Model A-M_w, and Model
 261 A-M_r were models incorporating the human mobility index in parks, workplaces, and
 262 residential based on Model A, respectively.

Model	Model formula	WAIC	MSE in LOOCV
Model A1	$\beta + \gamma + S + \alpha$	741.12	—
Model A2	$\beta + \gamma + S + f.w(R_t, 6) + \alpha$	727.31	—
Model A	$\beta + \gamma + S + f.w(R_t, 6) + f.w(T_t, 2) + \alpha$	681.60	0.63
Model A-M _p	$\beta + \gamma + S + f.w(R_t, 6) + f.w(T_t, 2) + m_p + \alpha$	677.92	0.65
Model A-M _w	$\beta + \gamma + S + f.w(R_t, 6) + f.w(T_t, 2) + m_w + \alpha$	658.89	0.46
Model A-M _r	$\beta + \gamma + S + f.w(R_t, 6) + f.w(T_t, 2) + m_r + \alpha$	651.87	0.37
Model A-M _r 1	$\beta + \gamma + S + f.w(R_t, 5) + f.w(T_t, 2) + m_r + \alpha$	666.57	—
Model A-M _r 2	$\beta + \gamma + S + f.w(R_t, 4) + f.w(T_t, 2) + m_r + \alpha$	668.37	—
Model A-M _r 3	$\beta + \gamma + S + f.w(R_t, 3) + f.w(T_t, 2) + m_r + \alpha$	664.26	—
Model A-M _r 4	$\beta + \gamma + S + f.w(R_t, 2) + f.w(T_t, 2) + m_r + \alpha$	671.56	—
Model A-M _r 5	$\beta + \gamma + S + f.w(R_t, 1) + f.w(T_t, 2) + m_r + \alpha$	669.79	—
Model A-M _r 6	$\beta + \gamma + S + f.w(R_t, 6) + f.w(T_t, 1) + m_r + \alpha$	653.22	—

263

264

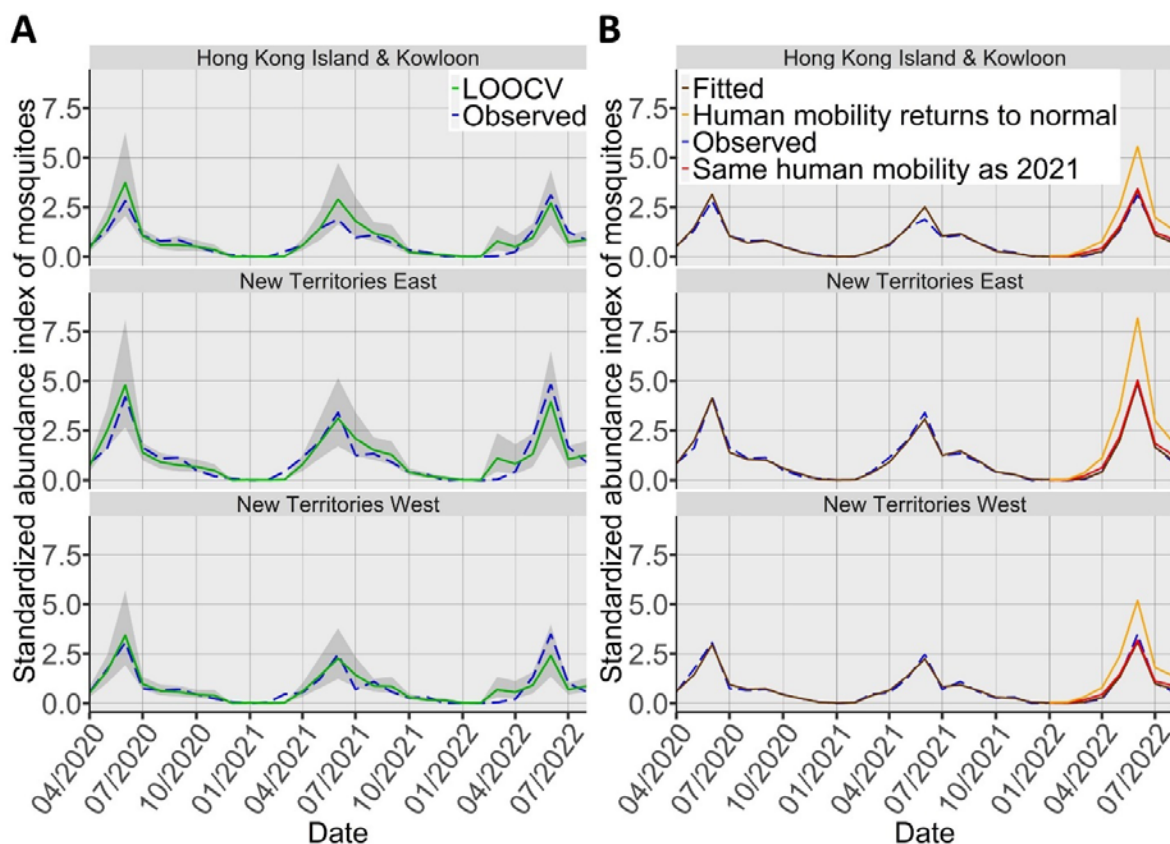
265 **Prediction of mosquito activity using weather and human mobility**

266 Overall, both models A-M_r and E-M_r showed similar predictive performances (Table 1 and
 267 Table S4), The model fit for mosquito abundance appeared to be slightly better than that for
 268 mosquito extensiveness as more observed data points in the year 2022 were within 95%
 269 confidence interval (CI) of the predicted values for mosquito abundance (Figure 3A and
 270 Figure S4A). It might be because mosquito abundance is more weather-related while
 271 mosquito extensiveness is more related to the presence of potential breeding places or the
 272 placement of the traps (Table 1 and Table S4).

273

274 The model estimated that residential mobility change has a negative effect on the mosquito
 275 abundance prediction (correlation coefficient = -0.075 (95%CI, -0.118--0.033); see Table S5).
 276 On the other hand, park mobility and workplace mobility had a positive effect on mosquito
 277 abundance. The effects of the human mobility indices on mosquito extensiveness were
 278 consistent with mosquito abundance.

279



280
281

282 **Figure 3 Comparison of observed and predicted results using the best model for**
 283 **mosquito abundance.** (A) Predicted results of mosquito abundance using leave-one-out
 284 cross-validation (LOOCV) with Model A-M_r. The grey shaded area represents the 95%
 285 confidence interval. The blue dashed line represents observed data and the green solid line is
 286 the leave-one-out cross-validation result. (B) Projected results of mosquito abundance in the
 287 year 2022 under different scenarios in human mobility (residential category): human mobility
 288 returns to the COVID-19 pre-pandemic period (orange) and the same human mobility as year
 289 2021 (red). The blue dashed line represents observed data and the brown solid line represents
 290 fitted data.

291

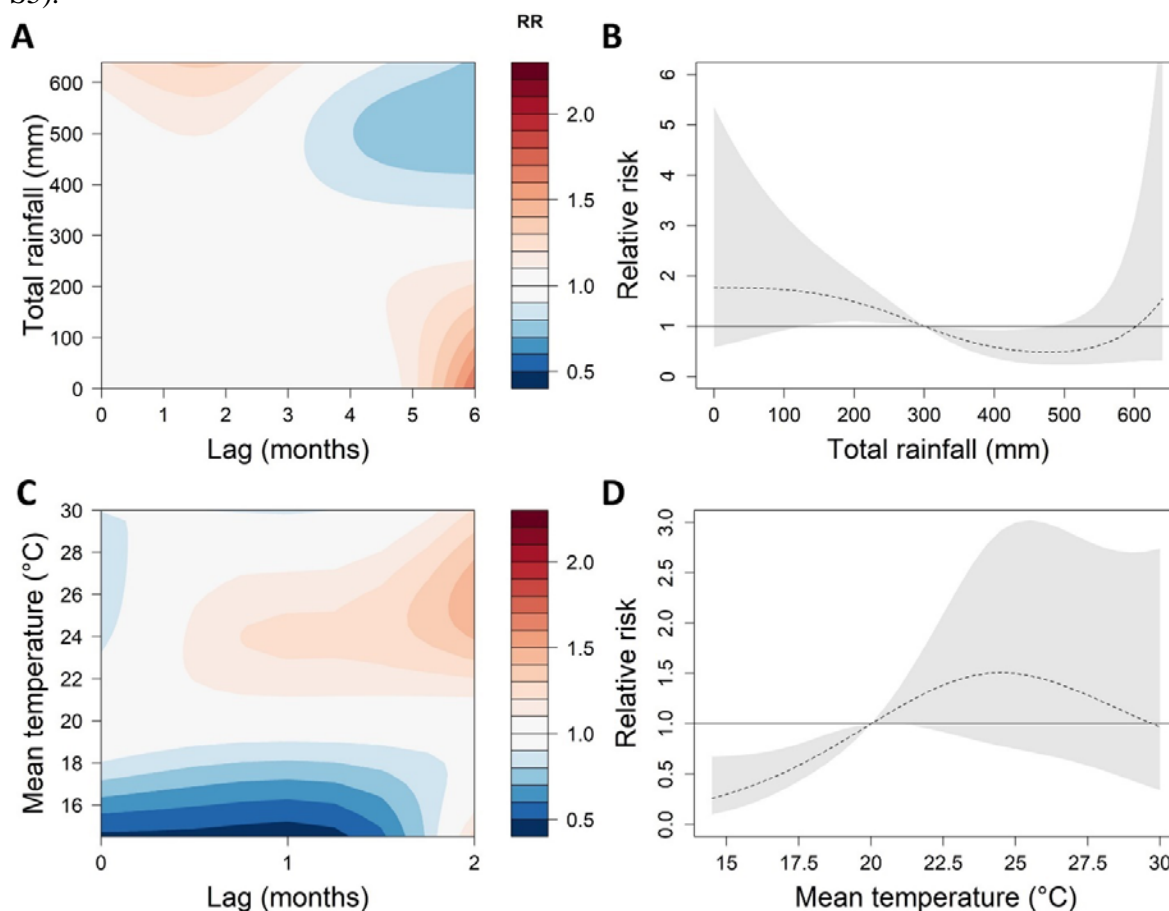
292 **Effects of weather conditions**

293 Higher relative risks in mosquito abundance were observed in the conditions of extremely
 294 low (<50 mm) or heavy rainfall (>500 mm) (Figure 4A). Compared with the reference (300
 295 mm), a reduction in total rainfall was associated with a higher relative risk (RR) after about
 296 4.5 months, reaching a maximum of 1.73 (95%CI, 1.19-2.51). However, heavy rainfall
 297 conditions (>500 mm) were associated with a higher RR within 3 months, reaching a
 298 maximum of 1.31 (95%CI, 0.99-1.73). When lagged effects were accumulated, the maximum
 299 RR occurred at no rainfall (Figure 4B). The accumulated RR decreased with total rainfall up
 300 to about 500 mm but increased again thereafter.

301

302 Compared with the reference mean temperature (20 °C), the warm conditions (21-30 °C) were
 303 associated with an increased risk of mosquito abundance after about half a month, leading to
 304 a maximum RR of 1.47 (95%CI, 0.94-2.32) at 25.5 °C (Figure 4C). When lagged effects were
 305 accumulated, the RR increased with mean temperatures from 15 °C to 26 °C but decreased at
 306 warmer conditions (>26 °C) (Figure 4D). The associations between total rainfall and mean

307 temperature with mosquito extensiveness were similar to that of mosquito abundance (Figure
308 S5).



309
310

311 **Figure 4 Effects of total rainfall and mean temperature on mosquito abundance using**
312 **the best model.** (A) Relative risk (RR) by total rainfall and lag months; (B) Cumulative RR
313 for total rainfall; (C) RR by mean temperature and lag months; (D) Cumulative RR for mean
314 temperature. The reference of total rainfall and mean temperature are 300mm and 20°C,
315 respectively. The deeper the shade of red, the greater the increase in RR compared with the
316 reference. The deeper the shade of blue, the greater the decrease in RR compared with the
317 reference. The black dashed line represents the cumulative exposure-response association.
318 The grey shaded area represents the 95% confidence interval.

319

320 **Model projections for human mobility change**

321 The model projected the mosquito abundance in two alternative scenarios for the year 2022: 1)
322 same residential mobility as before the COVID-19 Omicron wave, indicating returning to a
323 normal state, and 2) same residential mobility as year 2021, indicating a weak social
324 distancing. In the first scenario when human mobility returned to normal (before the COVID-
325 19 pandemic), cumulative mosquito abundance in all areas significantly increased by an
326 average of 80.49% compared to the actual situation. The cumulative mosquito abundance in
327 the HKK is increasing the most, at 83.41%. In the second scenario, cumulative mosquito
328 abundance in all areas was only slightly higher than the actual situation by an average of
329 10.96% (Figure 3B). The projection results of mosquito extensiveness were similar to those
330 of mosquito abundance (Figure S4B).

331

332 **Sensitivity analysis**

333 Prediction models in mosquito abundance and extensiveness were sensitive in the variable
334 selection of the lag of total rainfall, the lag of mean temperature, and the human mobility
335 indices (Table 1 and Table S4). Model A, the WAIC decreased from 681.60 to 651.88 after
336 adding the residential mobility index. When the total rainfall lag reduced from 6 months to
337 other lengths, WAIC increased. Similarly, When the mean temperature lag reduced from 2
338 months to 1 month, WAIC increased. The durations of lags in total rainfall and mean
339 temperature that produced the lowest WAIC for mosquito abundance and extensiveness were
340 selected.
341

342 **DISCUSSION**

343 **Influence of human mobility on mosquito activity**

344 Understanding the association between human mobility and mosquito activity helps in
345 forecasting the risk of DF transmission and developing effective strategies for its prevention.
346 Our results showed that residential mobility was negatively associated with mosquito
347 abundance, while mobility indices in parks and workplaces showed positive associations. The
348 results can be explained by that the increase in outdoor activities provides more chances to
349 feed meals (blood) to *Aedes albopictus* (6). The model projected that if human mobility (i.e.
350 residential) returned to normal in 2022, the risk of mosquito activity would increase
351 significantly (80% more) during the peak. In addition to border reopening (18), a possible
352 increase in mosquito abundance, extensiveness, and DF incidence might appear due to more
353 outdoor human activity.

354

355 Recently, Brady et al. also reported that Dengue incidence was associated with certain
356 Google human mobility indices (e.g. workplace mobility and park mobility) during the
357 COVID-19 period (3). The difference between their modelling results with our study may be
358 explained by some factors. The impact of human mobility may be different in mosquito
359 activity and Dengue incidence. Moreover, an increase in residential mobility may have
360 different impacts on mosquitoes between *Aedes Albopictus* and *Aedes Aegypti*, which are
361 both the main vectors to transmit DF. However, *Aedes Albopictus* was the only mosquito
362 vector found in Hong Kong. Those differences suggest that prevention of DF through vector
363 control should take into account the impact of human mobility on mosquito and Dengue
364 incidence simultaneously.

365

366 **Impact of total rainfall lags and mean temperature on mosquito activity**

367 Rainfall appeared to influence mosquito activity by different mechanisms. Both dry and wet
368 conditions were found to be associated with an increased risk of Dengue infection in China
369 (19). We found that heavy rainfall conditions (>500 mm) within 3 months were associated
370 with a higher risk of *Aedes* mosquito activity. On the other hand, low rainfall (<50 mm) was
371 associated with a higher risk with a longer lag (Figure 4A). A possible explanation is that
372 early low rainfall (around late winter or springtime) helps to maintain the number of
373 mosquito eggs or larval sites without the flushing effect (20). *Aedes albopictus* survives the
374 winter at its egg stage. When more rain comes in a warmer environment after a period of dry
375 conditions, there will be a large number of eggs hatching simultaneously leading to a bloom
376 in adult mosquitoes. This scenario can be particularly important when the mosquito begins to
377 grow, corresponding to the period from springtime to the pre-rainy season before the
378 monsoon in many subtropical regions in Asia (21). The results suggest that, in southern China
379 or its neighbourhoods, some extreme hydroclimatic events, such as delayed monsoon or
380 drought conditions, during springtime might increase the Dengue risk in summertime. Severe
381 drought conditions have been observed in spring in 2018 in Hong Kong, and 2015 and 2023
382 in Taiwan, followed by significant outbreaks (11,22,23).

383

384 In our findings, the mean temperature was positively associated with mosquito activity until
385 exceeding a threshold. We observed an increased mosquito activity risk after about a half-
386 month, similar to the time that *Aedes albopictus* may use to develop from eggs to adults. A
387 maximum level occurred about two months later when the mean temperature was between
388 25 and 26°C (Figure 4C). Our findings in Hong Kong were consistent with the previous
389 studies using Dengue incidence (9).

390

391 **Implications**

392 The spread of vector-borne diseases such as DF, Malaria, and Zika diseases can have serious
393 consequences for human health and even lead to large-scale deaths. Residential mobility
394 indicates the change in the time people spend at home, as the outcome of social distancing
395 measures during the COVID-19 pandemic period. Therefore, our results suggest that social
396 distancing measures may be an important intervention to reduce mosquito abundance.
397 Furthermore, our results indicate that knowing the impact of hydroclimatic events on these
398 diseases can provide important risk projections for the future. In vector control of South-East
399 Asia, the Global Vector Control Response prioritized enhancing vector surveillance,
400 forecasting, and monitoring effects of different factors (24). Extreme weather or
401 hydroclimatic events, such as heavy rains or droughts are happening more frequently in the
402 world (25). They might have critical influences on the dynamics of the mosquito population
403 depending on the time of their occurrences (26). Incorporating extreme hydroclimatic events
404 (such as drought conditions) together with human mobility patterns helps to forecast Dengue
405 risk and inform public health decisions in vector control for its prevention.

406

407 **Limitations and future works**

408 Several limitations exist within this study. The mosquito activity may also be influenced by
409 other human-induced factors, such as land use type and urbanization process (27,28). Control
410 measures may have been taken specifically around those Gravidtrap sites. But during the
411 zero-COVID period in Hong Kong, the impact of these mosquito control measures was
412 expected to be smaller. Furthermore, extreme weather events can affect a variety of climatic
413 factors, some of which might be important factors for mosquito activity, such as typhoons
414 (29). We chose two important weather factors according to the previous studies (1,8), instead
415 of considering all of them. Recent studies have assessed the impact of climate change on
416 Dengue risk (19,30). Incorporating the insights from our findings can provide a better
417 understanding of how extreme weather conditions and human mobility might influence the
418 Dengue vector's abundance and control.

419

420 **Conclusion**

421 As the COVID-19 pandemic ends and borders reopen, the risk of DF is expected to be higher
422 in many parts of the world. The study found that social distancing measures were associated
423 with reduced mosquito abundance and extensiveness. Furthermore, low rainfall was
424 associated with a higher risk of mosquito activity (abundance and extensiveness) with the 4.5
425 months lag (Figure 4A), which was able to explain the recent findings of the delayed effects
426 of weather conditions on Dengue incidence (9,10). The results suggested that the highest
427 Dengue risk after drought conditions was likely to be affected by the spread of Dengue
428 mosquitoes.

429

430 **Contributors**

431 YZ, KY and HY designed the study. YZ and KY developed the methods, performed the
432 research, and accessed and verified the data. YZ and KY wrote the initial draft of this
433 manuscript. YZ and HY contributed to the interpretation of the results. YZ, HY, and EW
434 helped revise the manuscript. All authors had full access to all the data in the study and had
435 final responsibility for the decision to submit for publication.

436

437 **Acknowledgements**

438 We thank Ming Wai Lee from the Food and Environmental Hygiene Department, the Govern
439 ment of HKSAR.

440

441 REFERENCES

- 442 1. Bhatt S, Gething PW, Brady OJ, Messina JP, Farlow AW, Moyes CL, et al. The global distribution and
443 burden of dengue. *Nature*. 2013;496(7446):504–507.
- 444 2. Liu B, Gao X, Ma J, Jiao Z, Xiao J, Hayat MA, et al. Modeling the present and future distribution of
445 arbovirus vectors *Aedes aegypti* and *Aedes albopictus* under climate change scenarios in Mainland
446 China. *Science of the Total Environment*. 2019;664:203–214.
- 447 3. Chen Y, Li N, Lourenço J, Wang L, Cazelles B, Dong L, et al. Measuring the effects of COVID-19-
448 related disruption on dengue transmission in southeast Asia and Latin America: a statistical modelling
449 study. *The Lancet infectious diseases*. 2022;22(5):657–667.
- 450 4. Yuan HY, Liang J, Lin PS, Sucipto K, Tsegaye MM, Wen TH, et al. The effects of seasonal climate
451 variability on dengue annual incidence in Hong Kong: A modelling study. *Scientific Reports*.
452 2020;10(1):4297.
- 453 5. Lee C, Vythilingam I, Chong CS, Razak MAA, Tan CH, Liew C, et al. Gravitrap for management of
454 dengue clusters in Singapore. *American Journal of Tropical Medicine and Hygiene*. 2013;88(5):888–
455 892.
- 456 6. Bonizzoni M, Gasperi G, Chen X, James AA. The invasive mosquito species *Aedes albopictus*: Current
457 knowledge and future perspectives. *Trends in Parasitology*. 2013;29(9):460–468.
- 458 7. Reinhold JM, Lazzari CR, Lahondère C. Effects of the environmental temperature on *Aedes aegypti* and
459 *Aedes albopictus* mosquitoes: A review. *Insects*. 2018;9(4):158.
- 460 8. World Health Organization. Dengue and severe dengue. 2023. Available at [https://www.who.int/news-](https://www.who.int/news-room/fact-sheets/detail/dengue-and-severe-dengue)
461 [room/fact-sheets/detail/dengue-and-severe-dengue](https://www.who.int/news-room/fact-sheets/detail/dengue-and-severe-dengue). (Accessed 17 March 2023)
- 462 9. Lowe R, Lee SA, Brady OJ, Bastos L, Colón-González FJ, on Climate Change C, et al. Combined
463 effects of hydrometeorological hazards and urbanisation on dengue risk in Brazil: a spatiotemporal
464 modelling study. *Lancet Planet Health*. 2021;5(4):e209–e219.
- 465 10. Lowe R, Gasparrini A, Van Meerbeek CJ, Lippi CA, Mahon R, Trotman AR, et al. Nonlinear and
466 delayed impacts of climate on dengue risk in Barbados: A modelling study. *PLoS Medicine*.
467 2018;15(7):e1002613.
- 468 11. Yuan HY, Wen TH, Kung YH, Tsou HH, Chen CH, Chen LW, et al. Prediction of annual dengue
469 incidence by hydro-climatic extremes for southern Taiwan. *International Journal of Biometeorology*.
470 2019;63:259–268.
- 471 12. Hong Kong Observatory. Climatological Information Services. Available at:
472 <https://www.hko.gov.hk/en/cis/climat.htm>. (Accessed 3 Jan 2024)
- 473 13. The Government of the Hong Kong Special Administrative Region. Summary of the Geographical
474 Constituencies. 2016. Available at <https://www.elections.gov.hk/legco2016/eng/maps.html>. (Accessed 3
475 Jan 2024)
- 476 14. Google. Community Mobility Reports. Available at <https://www.google.com/covid19/mobility/>.
477 (Accessed 3 Jan 2024)
- 478 15. Food and Environmental Hygiene Department. Vector-borne diseases. Available at
479 https://www.fehd.gov.hk/english/pestcontrol/dengue_fever/index.html. (Accessed 3 Jan 2024)
- 480 16. Gasparrinia A, Armstrong B, Kenward MG. Distributed lag non-linear models. *Statistics in Medicine*.
481 2010;29(21):2224–2234.
- 482 17. Vehtari A, Gelman A, Gabry J. Practical Bayesian model evaluation using leave-one-out cross-
483 validation and WAIC. *Stat Comput*. 2017;27:1413–1432.
- 484 18. Chen Y, Li N, Lourenço J, Wang L, Cazelles B, Dong L, et al. Measuring the effects of COVID-19-
485 related disruption on dengue transmission in southeast Asia and Latin America: a statistical modelling
486 study. *Lancet Infectious Diseases*. 2022;22(5):657–667.
- 487 19. Li C, Liu Z, Li W, Lin Y, Hou L, Niu S, et al. Projecting future risk of dengue related to
488 hydrometeorological conditions in mainland China under climate change scenarios: a modelling study.
489 *Lancet Planetary Health*. 2023;7(5):e397–406.
- 490 20. Seidahmed OME, Eltahir EAB. A Sequence of Flushing and Drying of Breeding Habitats of *Aedes*
491 *aegypti* (L.) Prior to the Low Dengue Season in Singapore. *PLoS Neglected Tropical Diseases*.
492 2016;10(7):e0004842.
- 493 21. Zhao S, Bei N, Sun J. Mesoscale analysis of a heavy rainfall event over Hong Kong during a pre-rainy
494 season in South China. *Advances in Atmospheric Sciences*. 2007;24:555–572.
- 495 22. Hong Kong Observatory. The Year's Weather-2018. 2019. Available at
496 <https://www.hko.gov.hk/en/wxinfo/pastwx/2018/ywx2018.htm>. (Accessed 3 Jan 2024)
- 497 23. Brendan Wong. Radio Taiwan International. Taiwan potentially facing worst drought in 30 years. 2023.
498 Available at <https://en.rti.org.tw/news/view/id/2009076>. (Accessed 3 Jan 2024)
- 499 24. Control of Neglected Tropical Diseases GMPHIEVC and R. Global vector control response: progress in
500 planning and implementation. 2020. Available at
501 <https://www.who.int/publications/i/item/9789240007987>. (Accessed 3 Jan 2024)

- 502 25. Fischer EM, Sippel S, Knutti R. Increasing probability of record-shattering climate extremes. *Nature*
503 *Climate Change*. 2021;11(8):689–695.
- 504 26. Liyanage P, Tozan Y, Overgaard HJ, Aravinda Tissera H, Rocklöv J. Effect of El Niño–Southern
505 Oscillation and local weather on *Aedes* vector activity from 2010 to 2018 in Kalutara district, Sri
506 Lanka: a two-stage hierarchical analysis. *Lancet Planetary Health*. 2022;6(7):e577–585.
- 507 27. Lee JM, Wasserman RJ, Gan JY, Wilson RF, Rahman S, Yek SH. Human activities attract harmful
508 mosquitoes in a tropical urban landscape. *Ecohealth*. 2020;17:52–63.
- 509 28. Yin S, Hua J, Ren C, Wang R, Weemaels AI, Guénard B, Shi Y, Lee T, Yuan H, Chong KC, Tian L.
510 Spatial pattern assessment of dengue fever risk in subtropical urban environments: The case of Hong
511 Kong. *Landscape and Urban Planning*. 2023;237:104815
- 512 29. Kao B, Lin CH, Wen TH. Measuring the effects of typhoon trajectories on dengue outbreaks in tropical
513 regions of Taiwan: 1998–2019. *International Journal of Biometeorology*. 2023;67:1311–1322.
- 514 30. Gibb R, Colón-González FJ, Lan PT, Huong PT, Nam VS, Duoc VT, et al. Interactions between climate
515 change, urban infrastructure and mobility are driving dengue emergence in Vietnam. *Nature*
516 *Communications*. 2023;14(1):8179.
- 517